13

Enabling Technologies for Multi-Gigabit Wireless Communications in the E-band

Val Dyadyuk, Y. Jay Guo and John D. Bunton
CSIRO ICT Centre
Australia

1. Introduction

High data rate millimeter-wave communication systems are of growing importance to the wireless industry. This can be attributed partly to an ever-increasing demand for bandwidth and scarcity of the wireless spectrum, and partly to the decreasing cost of millimetre-wave monolithic integrated circuits (MMIC) which make transmitting and receiving devices cheap to produce. Gigabit Ethernet (GbE) has become a standard protocol for the wired data transmission and usage of 10 Gigabit Ethernet (10GbE) is rapidly increasing. While known fiber optic data transfer devices can provide multi-gigabit per second data rates, infrastructure costs and deployment time can be prohibitive for some applications. Rapidly deployable, low cost wireless links can compliment the fiber networks bridging the network gaps. Multi-gigabit wireless applications include backhaul and distributed antenna systems for the 3G/4G mobile infrastructure, enterprise connectivity, remote data storage, wireless backhaul for the Wireless Local Area Networks (WLAN) and the short range wireless personal area networks (WPAN). Wide license-free spectrum around 60 Gigahertz (GHz) is allocated in most countries worldwide. While mainstream research is focused on development of multi-gigabit short range WPAN for consumer-level applications (Yong and Chong, 2007), commercial point-to-point links in the 60 GHz band with data rates up to 1.25 Giga bits per second (Gbps) are also available from several manufacturers. However, high propagation loss due to oxygen absorption in this band and regulatory requirements limit the communication range for outdoor applications. The recent allocation of the E-band spectrum (71-76 and 81-86 GHz) in USA, Europe, Russia and Australia provides an opportunity for line of sight (LOS) links with longer range and higher data rates, ideally suited for fiber replacement and backhaul applications. Current E-band commercial point-to-point wireless links[1,2,3], are limited to speeds up to 1.25 Gbps and use simple modulation techniques like amplitude shift keying (ASK) or binary phase shift keying (BPSK) with spectral efficiency below one bit per second per Hertz (bit/s/Hz).

---

1 [Online]: http://www.bridgewave.com/products/80GHz.cfm
2 [Online]: http://www.loeacom.com/Loea_2710_DataSheet-0508.pdf
3 [Online]: http://www.proxim.com/downloads/products/gigalink/DS_0407_Gigalink_US.pdf

A research prototype of the E-band multi-gigabit data rate wireless communication system that uses a multi-level digital modulation has also been developed (Dyadyuk et al., 2007d). The proposed method is applicable to systems where the radio channel bandwidth is greater than the Nyquist spectral width of the associated A/D and D/A converters. Such systems can be utilized for the E-band full-duplex wireless links with a spectral efficiency scalable from 2.4 to 4.8 bit/s/Hz for 8-PSK to 64-QAM modulations to transmit 12 to 24 Gbps. This has been proven by experimental results on the 6 Gbps prototype with spectral efficiency of 2.4 bit/s/Hz. According to our knowledge this is the highest spectral efficiency achieved to date for a millimeter wave link with a demonstrated data rate above 2.5 Gbps.
While the spectrum available in the E-band allows for the multi-gigabit-per second data rates, the achievable communication range is limited by several factors, which include atmospheric attenuation and the output power attainable by semiconductor devices due to physical constraints. Currently achievable communication range of the E-band wireless networks under various propagation conditions are evaluated in this chapter using analytical estimates and experimental results. It is shown that the performance of the fixed and ad-hoc mm-wave networks for existing and emerging applications can be further improved by implementation of the spatial power combining antenna arrays.
The main challenges in the practical realization of the proposed systems, specifically the mm-wave front end integration and computationally efficient digital signal processing methods are also discussed. In this chapter we discuss enabling technologies and challenges in the commercial realization of such systems, possibilities of further improvement of fixed wireless links performance and feasibility of the development of future ad-hoc or mobile wireless networks in the E-band.

2. Multi-gigabit links for fixed terrestrial wireless networks

2.1 Spectrally efficient multi-gigabit link

The state of the art multi-gigabit wireless technology to date has been reported in our works (Dyadyuk et al., 2007a, 2007b, 2007c, and 2007d). The proposed system solution is suitable for wireless communication systems with data rates beyond 20 Gbps. We have proposed a frequency-domain multi-channel multiplexing method[4] for improved spectral efficiency, designed a 12 Gbps system in the E-band, and built a four–channel 6 Gbps concept demonstrator. With 8PSK (phase shift keying), we achieved a spectral efficiency of 2.4 bit/s/Hz. This is the highest spectral efficiency achieved to date for a millimeter wave link with a demonstrated 6 Gbps data rate. The proposed method is applicable to systems where the radio channel bandwidth is greater than the Nyquist spectral width of the associated A/D and D/A converters. As commercially available, reasonably priced analogue-to-digital (A/D) and digital-to-analogue (D/A) converters can not operate at multi-gigabit per second speeds, digital channels operating at a lower sampling speed were used. For a single carrier modulation, the proposed frequency-domain channel multiplexing technique[4] uses the root-raised-cosine digital filters (RRC) to eliminate data aliases and relaxed frequency-response requirement of analogue anti-aliasing filter. This technique allows contiguous channels to

[4] Bunton, J. D.; Dyadyuk, V.; Pathikulangara, J.; Abbott, D.; Murray, B.; Kendall, R. "Wireless frequency-domain multi-channel communications". Patent application WO2008067584A1, IPC H014B1/04, H04L27/26, H04B1/06 (Priority 5 Dec 2006), 12 June 2008

abut each other without the need for guard bands and makes the efficient use of wireless spectrum. While prototype system used converters with 2 Gbps sampling speed, currently available A/D and D/A can operate at the sampling speed up to 5 Gbps reducing the number of sub-channels by the factor of 2.

A simplified block diagram of the system (Dyadyuk et al., 2007d) that uses a spectrally efficient digital modulation is shown in Figure 1. The system includes a digital interface, a digital modem, an intermediate frequency (IF) module and a wideband millimeter-wave front end having transmit and receive sections and a high-directivity antenna.

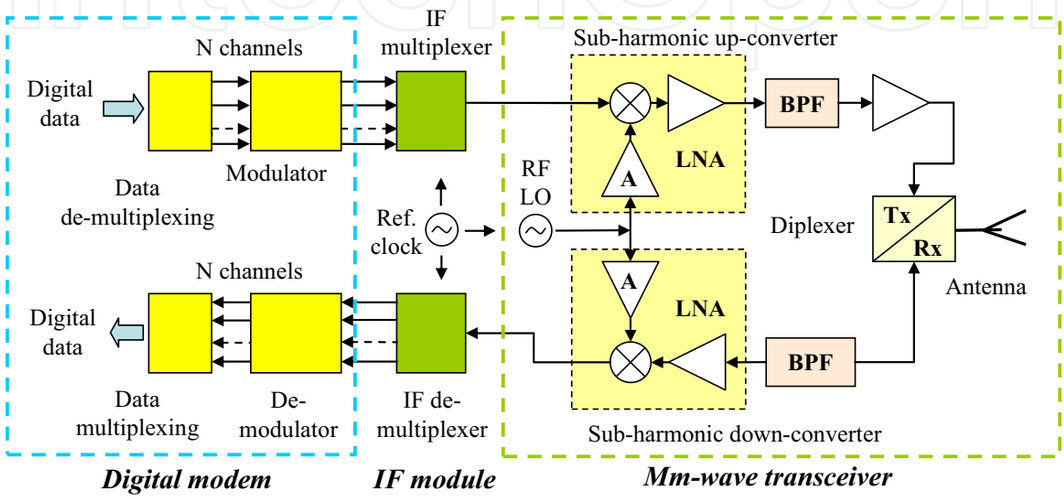

Fig. 1. Generalized block-diagram of the system

At the transmitter (Tx) input digital data stream is de-multiplexed into N digital channels (e.g. four to sixteen). At the modulator each digital channel was processed in a field-programmable gate array (FPGA) to generate the transmit symbols together with pre-compensation[5]. High speed D/As generate the analogue intermediate frequency (IF) signal for each channel in the second Nyquist band. The bands are translated in frequency and combined with the band edges abutting. No guard bands are needed because of the spectral limiting imposed by the modulation. Combined IF signal with the bandwidth equal to N •BWo is up-converted into the mm- wave carrier frequency, amplified and transmitted over a line-of-sight path.

At the receiver (Rx), received signal is down-converted from the millimeter-wave carrier frequency into IF and de-multiplexed in frequency domain into N sub-channels, then sampled by the high-speed analogue-to-digital converters (A/D) and de-coded by the FPGA that implements matched RRC filters on the *N* digital channels, these can be multiplexed into a single digital stream where required.

[5] Bunton, J. D.; Dyadyuk, V.; Pathikulangara, J.; Abbott, D.; Murray, B.; Kendall, R. "Wireless frequency-domain multi-channel communications". Patent application WO2008067584A1, IPC H014B1/04, H04L27/26, H04B1/06 (Priority 5 Dec 2006), 12 June 2008

For the prototype system with eight digital channels a total throughput of 12 Gbps is achieved. This can be used to implement the digital interface is either a 10 gigabit Ethernet interface together with forward error correction (FEC) on the channel. Alternatively each channel can be used to implement 1 Gbps Ethernet with FEC on the channel.

2.2 Wideband millimeter-wave transceiver

The signal to noise or interferer ratio (SNIR) required for a given BER increases with the increase in order of the multi-level digital modulations. Therefore, transceivers which can provide a high signal-to-noise ratio performance are required.

The key mm-wave transceiver in the system shown in Figure 1 uses heterodyne architectures with sub–harmonic frequency translation. Implementation of the sub-harmonic local oscillator (LO) allows a reduction in the complexity and cost of a transceiver. While a sub-harmonic mixing incurs a small penalty of a several dB in conversion gain or dynamic range, it provides a benefit of inherent suppression of both fundamental and even harmonics of the LO and down-converted LO noise.

The key element of the transceiver suitable for systems employing multi-level digital modulations is a sub-harmonically-pumped frequency converter that uses the second or fourth LO harmonic. The disadvantages compared with a fundamental LO mixer, are the slightly higher conversion loss (of about 2 dB for the 2nd harmonic), narrower bandwidth and the slightly lower conversion gain at 1dB compression level.

One convenient way to implement the architecture shown in Figure 1 entails the use of a common 39.25 GHz LO source for both receive and transmit circuits. Thus, both the 71-76 GHz and the 81-86 GHz bands can be utilized for a full-duplex communication system using the lower or upper side-band conversion in each chosen (receive or transmit) direction.

The recent progress in Si CMOS technology has largely been driven by the 60 GHz WPAN activities. Currently, the SiGe HBT and BiCMOS MMICs are the most likely candidates for high-volume 60 GHz WPANs as the reported chip sets (Cathelin et al., 2007; Floyd et al., 2007; Grass et al., (2007); Pfeiffer et al., 2008; Reynolds et al., 2007) meet current system specifications for the WPAN transceivers. This may lead to development of low-cost fully-integrated transceivers in the near future.

However, silicon chip sets suitable for the 71-76 and 81-86 GHz are not yet available. Currently, the LO driver amplifier can be built using SiGe BiCMOS, but the PA with a desired P1dB output compression of above +20 dBm are feasible only in Gallium Arsenide (GaAs) technology. Low noise SiGe amplifiers suitable for wide-band receivers have not been reported yet in the W-band.

Wide-band receive and transmit integrated modules with sub-harmonic frequency translation which were developed using a GaAs MMIC chip set have been reported in (Dyadyuk et al., 2008a, 2008b).

Figure 2 shows a photograph of the down-converter integrated into a metal housing using a traditional wire-bond approach. The LO input and the IF outputs are coaxial. The RF input uses a WR10 waveguide and an adjustable waveguide-to-microstrip transition.

The chipset includes a commercially available LNA (ALH459, Velocium, Hittite Microwave), a V-band driver amplifier (Archer and Shen, 2004) that uses a 0.15μm GaAs pHEMT process), and a sub-harmonically-pumped image-reject mixer (Dyadyuk et al., 2008a). The mixer was built using two anti-parallel pairs of 1x5 μm GaAs Schottky diodes (a standard commercial process available from United Monolithic Semiconductors).

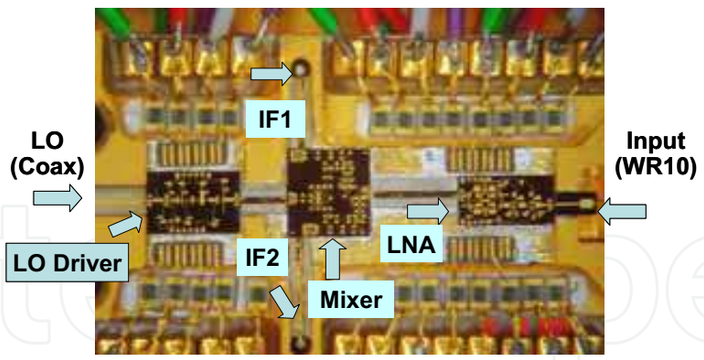

Fig. 2. Photograph of the integrated down-converter

Figure 3 shows the measured performance for an image-reject configuration using an external 90º hybrid (Krytar Model 1831). The measured image rejection was above 16 dBc. The LO power was about -9 dBm at the input to the module. The Noise Figure is estimated to be below 7.5 dB based on measured MMIC data and the insertion loss of the package inter-connects. The module exhibits extremely wideband performance with a -3 dB bandwidth greater than 9 GHz in both upper and lower side-bands.

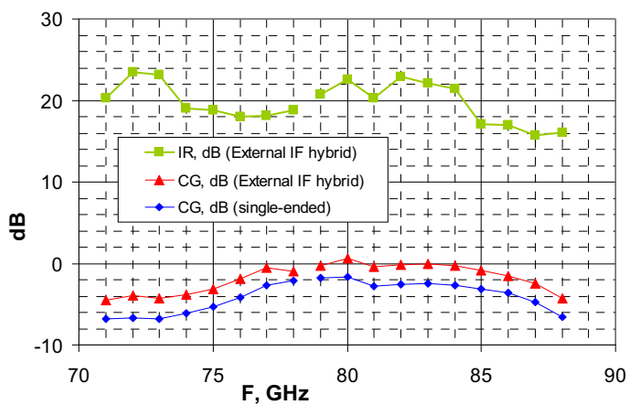

Fig. 3. Measured performance of an integrated down-converter module at the LO of 39.25 GHz in a single ended and image-reject configurations

Measured input and output P1dB compression was above -14 and -18 dBm respectively. Other experiments show that in the RF frequency range of 70 to 88 GHz the performance of the down-converter can be further optimized for a range of LO frequencies from 37 to 42 GHz resulting in a -3 dB bandwidth greater than 7 GHz in a chosen sideband.

The transmit module was integrated in a similar fashion using the same MMIC chip set with the LNA ALH459 MMIC at the output of the up-converter. The measured performance is shown in Figure 4 for a single IF port and image-reject configurations. The LO power was about -7 dBm at the input to the module. Measured 1 dB compression of the conversion gain at the IF input and RF output was above -14 and -18 dBm respectively.

An image-reject performance was measured combining the input IF ports in an external 90º hybrid (Krytar Model 1831). Measured image rejection was above 16 dBc. The measured -3

dB RF bandwidth was above 7 GHz and 5 GHz respectively in the upper and lower side-bands.

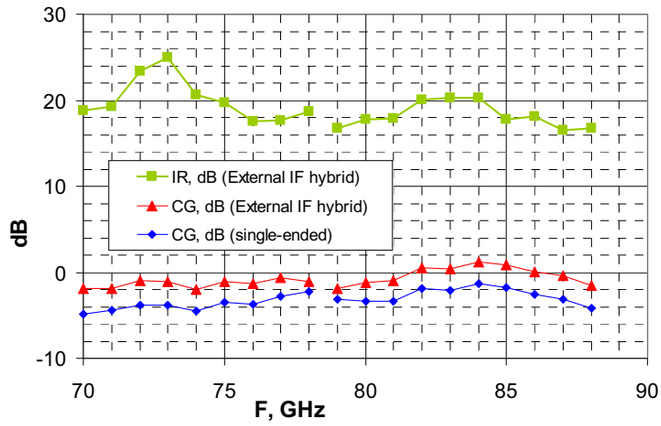

Fig. 4. Measured performance of an integrated up-converter module at the LO of 39.25 GHz in a single ended and image-reject configurations

The performance of the up-converter can be further optimized in the RF frequency band from 70 to 88 GHz for a range of LO frequencies from 37 to 42 GHz resulting in a -3 dB bandwidth of more than 7 GHz in a chosen sideband.

2.3 Frequency-domain multiplexing technique

Frequency-domain multiplexing commonly uses analogue filters that require frequency guard bands between adjacent radio channels, which is an inefficient use of the available bandwidth. The proposed method [Dyadyuk et al., 2007d] is applicable to systems where the radio channel bandwidth is greater than the Nyquist channel width of the associated A/D and D/A converters. It entails a novel frequency-domain channel multiplexing technique that combines the root-raised-cosine digital filters (RRC) to eliminate data aliases and relaxed frequency-response linear-phase analogue pass-band filters to reject only unwanted Nyquist responses without the need for guard bands.

The input binary data is de-multiplexed into N identical digital channels. A pre-compensated digital modulator is implemented in a field-programmable gate array (FPGA). Uncompensated symbols have the form of an impulse response of an RRC filter. This eliminates data aliases, and relaxes the requirements to band-pass filters (BPF) that can have up to 30% transition bands to reject unwanted Nyquist responses.

For simplicity, we describe this solution for a Return to Zero (RTZ) type of D/A converter operating at the sampling clock frequency of Fs to generate the wanted analogue signal in the second Nyquist zone. A Sync function envelope arising from the sampling by a return-to-zero (RTZ) D/A has the first zero at the double of the sampling frequency Fs. At the chosen symbol rate of Fs/4, the analogue data signal in the wanted Nyquist zone is band limited to $0.25 \bullet Fs \bullet (1+a)$, where a is a roll-off factor of the RRC filter, and outside this band the signal power is practically zero. The truncation of the impulse responses leads to some but low level residual power outside the wanted Nyquist zone.

The transmit sections of the system that implements the guard-band-free frequency-domain multiplexing of N high-speed digital channels (bandwidth of BWo each) into a single RF channel is shown in Figure 5.

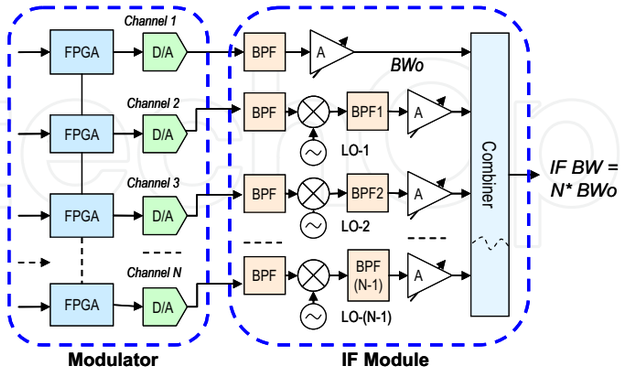

Fig. 5. The modulator and IF modules of the transmitter

The concept of combining an analogue band-pass filter (BPF) and a RRC pulse s haping filter for frequency–domain multiplexing is illustrated in Figure 6.

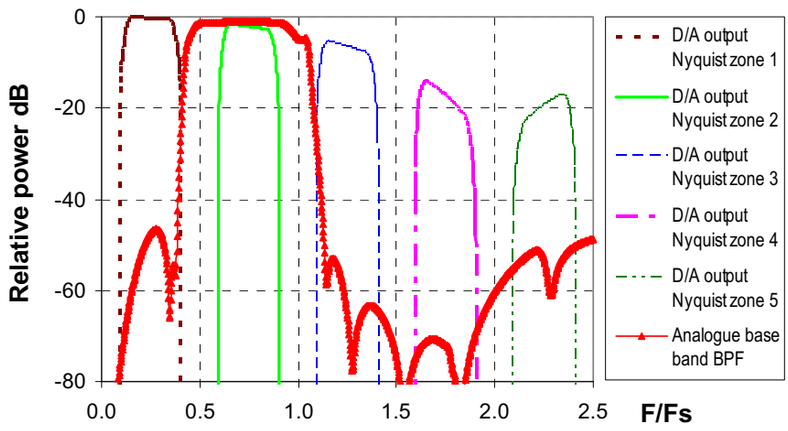

Fig. 6. First five images at the output of a RTZ D/A converter and a frequency response of a typical analogue BPF.

Figure 6 shows a D/A output in first five Nyquist zones and a typical uncompensated frequency response of an analogue BPF aligned with the second Nyquist zone. Channel 1 is directly generated by a RTZ D/A and the subsequent N-1 channels are up-converted to abut each other using frequency translation in a BWo step. Identical analogue "base band" BPF with a frequency response shown in Figure 6 is used for each digital channel at the D/A outputs. Band-pass filters BPF1 to BPF(N-1) shown in Figure 5 eliminate images arising from the frequency translation. The LO frequencies are selected to avoid unwanted mixing terms in the pass bands of neighbouring channels. This technique of using digital filters with

sharp cut-off along with the analogue band-pass filters allows contiguous channels to abut each other and allows efficient use of wireless spectrum.
A receive section that implements de-multiplexing of a receive channel into N high-speed digital channels is shown in Figure 7. The received signal is down- converted from the mm-wave carrier frequency into IF and de-multiplexed in the frequency domain into N sub-channels, then sampled by the high-speed analogue-to-digital converters (A/D), and de-coded by the FPGA that implements matched RRC filters. The de-multiplexer employs analogue filters BPF and BPF1 to BPF(N-1) identical to the filters used in the multiplexer. Data from the N digital channels can be multiplexed into a single digital stream.

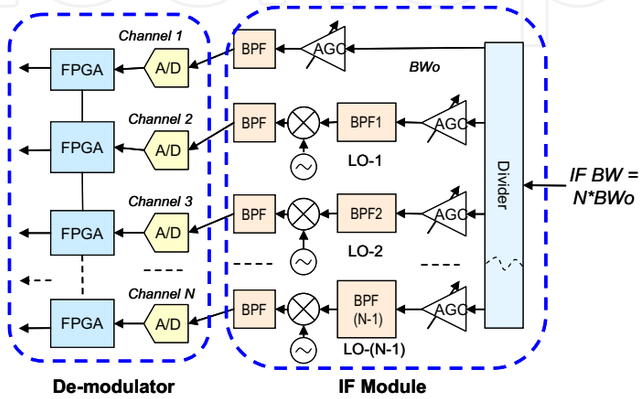

Fig. 7. The de-modulator and IF modules of the receiver

The digital modulator and demodulator are implemented in FPGAs. The FPGA logic runs at an effective sample rate Fs due to a multi-lane and parallel implementation of circuits.
The modulator stores a digital representation of the pre-compensated transmit signal for every symbol for 32 symbol periods. The symbols enter a shift register of length 32, and each of these symbols generates one set of samples from the stored representations to the output at the appropriate time. An adder chain produces the modulator waveform and the D/A converter produces the analogue IF signal. The D/A converters have a sufficient effective number of bits to accommodate this pre-compensation without degrading SINR. This novel technique is computationally efficient as no multiplications are required. Its complexity is low and grows linearly with the length of pre-compensation. The 32-symbol length modulator is sufficient to pre-compensate group delay ripple of several nanoseconds. Another innovative feature of this symbol to signal transform is that it incorporates conversion to intermediate frequency (IF), and a pre-compensated RRC filter. A chirp based channel sounding determines the pre-compensation required for the transmit symbols.
On the receive side, the FPGA digitally down converts the data from an A/D converter to the baseband quadrature (I and Q) signals. The low pass filter associated with the down converter is the RRC filter. This digital filter with a sharp cut-off rejects the out of band noise generated by frequency domain multiplexing scheme. One novel feature of this RRC filter is that it can interpolate the output sample time instant to a resolution of 1/32 of the symbol period. A bit centre tracking circuit controls the RRC sampling instant. The other blocks of the demodulator include constellation de-rotation circuits, symbol decoder, symbol insertion and deletion circuits to account for symbol rate mismatch between the transmitter and the receiver and the symbol to bits converter.

2.4 System capacity and performance

For the proposed system, the practically achievable SINR is limited by several factors. They include the LO phase noise, the limited linearity of power amplifiers (PA), inter-channel interference and the limited signal to noise and distortion ratio (SINAD) of the high speed converters over wide band pre-compensated channels. The maximum data rate is the product of the bandwidth BW and spectral efficiency E=k /(1+a), where k is the number of bits per symbol, and a is the excess bandwidth (or roll-off factor) of the root-raised-cosine (RRC) filter. The SINR required for a given BER increases with increased order of a multi-level digital modulation. Thus the SINR above 36 dB is required for k≥ 8. Whereas the phase noise of the oscillators increases with frequency, commercially available phase-locked DRO sources are suitable for the multi-level modulations. Thus, the phase noise integrated over the channel bandwidth was below – 46 dBc for the 39-42 GHz oscillators tested in the prototypes. This level is adequate for the modulations with k ≤ 8 (e.g. including 256 QAM). The measured SINAD for the commercial 2 Gsps D/A was about 50 dB for an ideal analogue channel. This was further reduced to about 40 dB for a typical physical channel. The SINAD for the A/D was measured to be about 35 dB. An approximate estimate that includes the above figures, the noise of the low-noise amplifiers, linearity of the PA and the residual inter-channel interference results in a practically attainable signal to noise or interferer ratio SINR of about 32 dB at the carrier frequency 71-86 GHz. Therefore the maximum realistic modulation order would be k ≤ 6 (e.g. 64 QAM) with E ≤ 4.8 bits/s/Hz for a typical roll-off factor of 0.25.

This leads to the conclusion that the system configuration described above can be utilized for wireless links with a spectral efficiency scalable from 2.4 to 4.8 bit/s/Hz for 8-PSK to 64-QAM modulations to transmit 12 to 24 Gbps over 5 GHz wireless bandwidth and up to 48 Gbps over 10 GHz of bandwidth.

A small-scale four-channel concept demonstrator of this system has been built using Xilinx FPGAs, Euvis model MD653 RTZ D/A converters and Atmel A/D converters operating at 2 Giga samples per second (Gsps). Four identical digital channels were multiplexed into a single 2.5 GHz wide IF signal using an optimal combination of the root-raised-cosine digital filters and linear-phase analogue filters. The base band signal bandwidth was 625 MHz at a symbol rate of 0.5 giga symbols per second and the RRC roll-of factor of 0.25. The aggregate link data rate was 6 Gbps at 2.4 Bit/s/Hz spectral efficiency for the 8PSK modulation over a 2.5 GHz width radio channel in the 81-86 GHz band.

The prototype has been installed at the 250 m long test range in Sydney, Australia. At this range a very low transmitted power of 0.25 mW was sufficient to provide link margin above 10 dB for a 99.999% annual availability at the range location at the raw bit error rate (BER) below 10^{-7}.

A separate video transmission experiment has been carried out to evaluate the link performance with a forward error corrected payload. In this experiment, sixteen video streams were aggregated into a GbE physical layer format (GMII) using multiple PCs and switches. The aggregated data of about 1.25 Gbps was transmitted over one of the digital channels using a Reed Solomon 200/216 FEC. The other three channels were used for raw BER measurements and channel sounding experiments. The video streams were generated by video cameras and DVD players. A sample of the payload received over the link is shown in Figure 8.

Fig. 8. Sample of a digital video payload received over a channel of the 6 Gbps link.

The forward-error-corrected video image was received without a loss of data or visible distortions at SINR ≥ 12 dB. This was measured with the RF path blockage of approximately 18 dB introduced by an additional RF attenuator inserted between the diplexer and antenna. The corresponding raw BER was measured on the other channels using a 1.5 Gbps Gray-coded pseudo-random 8PSK sequence. The raw BER was less than $2 \cdot 10^{-2}$.
Test results of a concept demonstrator with 6 Gbps aggregate data rate in the 81-86 GHz band and 2.4 bit/s/Hz spectral efficiency have validated the proposed system concept. In this chapter, we have chosen the above prototype as a reference point-to-point link in the predictions of the communication range of high data rate millimeter-wave communication systems.

3. Mm-wave propagation and communication range

Using the well known Frii's transmission formula, the available communication range R [km] can be determined as a root of a non-linear equation

$$P_T+G_T+G_R-10 \bullet \log (kTB)- NF- SINR-L_0-L_m- 92.45- 20 \bullet \log(R)-A \bullet R - 20 \bullet \log(F) =0 \qquad (1)$$

where P_T is transmitted power in dBW, A is the specific atmospheric attenuation in dB/km, G_T and G_R are effective gains of the receiving and transmitting antennas in dBi, k is the Boltzmann constant, T is temperature in ^oK, B is bandwidth of the receiver in Hz, NF is the noise figure of the receiver in dB, where SINR is the signal to interference and noise ratio in dB required for a certain BER by the modulation method, L_0 includes antenna pointing loss and other expected loss in dB, L_m is the minimum specified link margin in dB, and F is the frequency in GHz. The last four terms determine the LOS link free space loss.

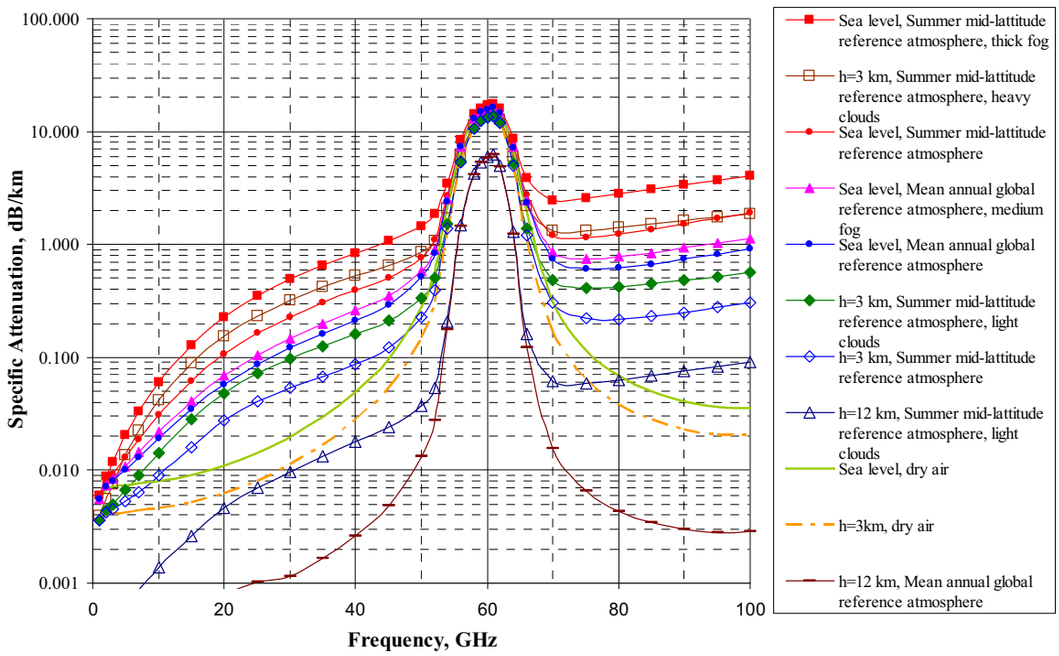

Fig. 9. Specific attenuation (in the absence of precipitation) for selected atmospheric conditions for the frequency range 10 - 100 GHz

Due to the short wavelength at mm-wave frequencies, a high gain antenna with a small physical size can be conveniently used to increase the communications range and to reduce interference with other systems. Attenuation by atmospheric gases at a specific radio frequency depends on the atmospheric conditions such as barometric pressure and temperature (both are functions of the altitude), humidity, and density of water droplets in clouds or fog. Specific attenuation A [dB/km] calculated for a horizontal path at typical atmospheric conditions at sea level and altitude h of 3 and 12 km using the ITU Recommendations[6] is given in Figure 9. Altitudes of 3 and 12 km are chosen to illustrate atmospheric attenuation for the aircraft-to-aircraft communication systems. Two standard reference atmospheres (the mean annual global reference atmosphere and the summer mid-latitude reference atmosphere) with water vapour density at sea level of 7.5 and 14.35 g/m^3 respectively are used to calculate the data given in Figure 9. Additional attenuation due to clouds and fog is estimated in accordance with the ITU Recommendation ITU-R.P.840-3 for medium fog or light clouds (visibility of the order of 300m) and thick fog or heavy clouds (visibility of the order of 50m).

It is well known that with the exception of the 60 GHz band (56-64 GHz, where radio propagation is affected by the atmospheric oxygen resonant absorption), specific attenuation increases with increasing water vapour and droplets density. In the absence of precipitation, moderate specific attenuation at the E-band (below 3 dB/km) makes this band suitable for medium and long range both terrestrial and elevated tropospheric paths. While the path loss is lower at the lower frequency, there is no current appropriate spectrum allocation at the

[6] ITU-R.P.676-7; ITU-R.P.840-3; ITU-R.P.510-10

frequencies below 56 GHz with the instantaneous RF bandwidth required for the multi-gigabit data rates.

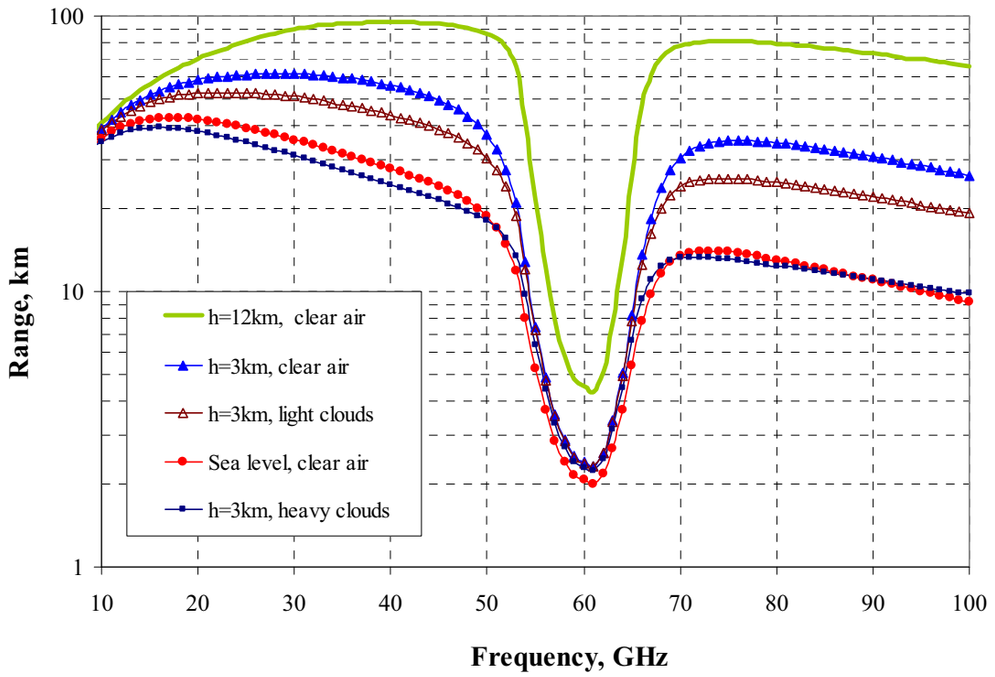

Fig. 10. Estimated communication range for a typical link with 0.36m diameter fixed beam antennas at the carrier frequency range 10 to 100 GHz

The estimated communication range for a typical configuration of the line-of-sight link equipped with identical fixed beam antennas (having a circular aperture 0.36 m diameter) is given in Figure 10 for the operating frequency from 10 to 100 GHz. For simplicity and comparison with the earlier reported results, we use a reference point-to-point link with the specification equivalent to a single 1.5 Gbps channel of the 6 Gbps prototype described above in Section 2.4 with the exception of the carrier frequency, the antenna size and transmitted power. We have assumed that a transmitter uses a single commercial power amplifier MMIC. As the data in Figure 10 was calculated for a very wide frequency range, we used linear approximation (Dyadyuk and Guo, 2009) for the output power and the receive noise figure based on the specifications of commercially available MMICs. Link margin Lm is 3dB at the bit error rate below 10^{-7} for the 8PSK. Figure 10 shows that the communication range available for the chosen link scenario does not change significantly between 10 and 100 GHz (except the 60 GHz band) at the favourable atmospheric conditions.

Hence, the frequency can be increased to take advantage of wide band operation and less interference, to achieve higher data rates over a reasonable link distance.
The main factor that limits available communication range at mm-wave frequencies is the fading due to rain. For illustrative purposes, the specific attenuation by rain Ar calculated in

accordance with the ITU-R Recommendation for vertical polarization is shown in Figure 11. The rainfall rate exceeded for a given probability of the average year for each specific location can be obtained from the ITU_R Recommendation ITU-R.P.837-5. Data Figure 11 indicates that in the upper E-band (vertical polarization) the attenuation Ar exceeds 11 dB/km and 18 dB/km respectively for heavy rainfalls of 25mm/hr and 50mm/hr.

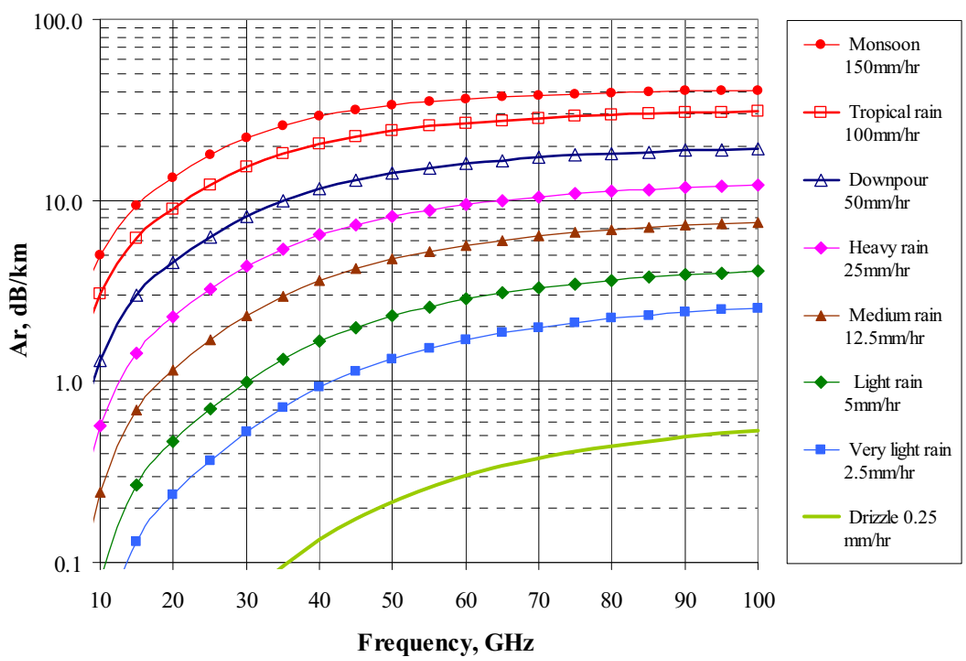

Fig. 11. Specific attenuation Ar [dB/km] due to rain (vertical polarization)

Predicted communication range for the 10 Gbps system described in Section 2 at a given rain rate is shown in Figure 12 for the carrier frequency of 83.5 GHz and 52 dBi antenna gain.
Total attenuation over a LOS path includes attenuation by atmospheric gases and rain. Multipath effects and sub-path diffraction are not modelled. The propagation model used here includes the path length reduction factor recommended by the ITU-R.P.530-12 to account for an effective rain cell size at given rain intensity and an effective path length (as rain, particularly intensive rain, is not distributed homogeneously). It is noted that the above method is recommended to 40GHz only and its use above that frequency has not been tested.
The minimum range was estimated for the BER not exceeding 10^{-7}. Adaptive modulation and appropriate forward error correction techniques can be used for operation over longer paths.
At a conservative estimate (with operating frequency selected in the upper E-band (81 – 86 GHz), and the output power of 17 dBm available from a commercial MMIC) available communication range at 10 Gbps data rate exceeds 4 km at the rain rate up to 100 mm/hr. The range can be increased using the transmit power level up to the regulatory limit of 33

dBm. The rainfall rate exceeded for a given probability of the average year can be obtained from the ITU_R Recommendation[7] for each specific location.
During more than 99.9% of the average year, very high data rate transmission over 7 – 10 km is feasible in most locations. As intensive rain events periods are very short for most locations excluding the tropical areas, required range can be maintained during these periods by using an adaptive modulation with reduced data rate as shown in Figure 12.

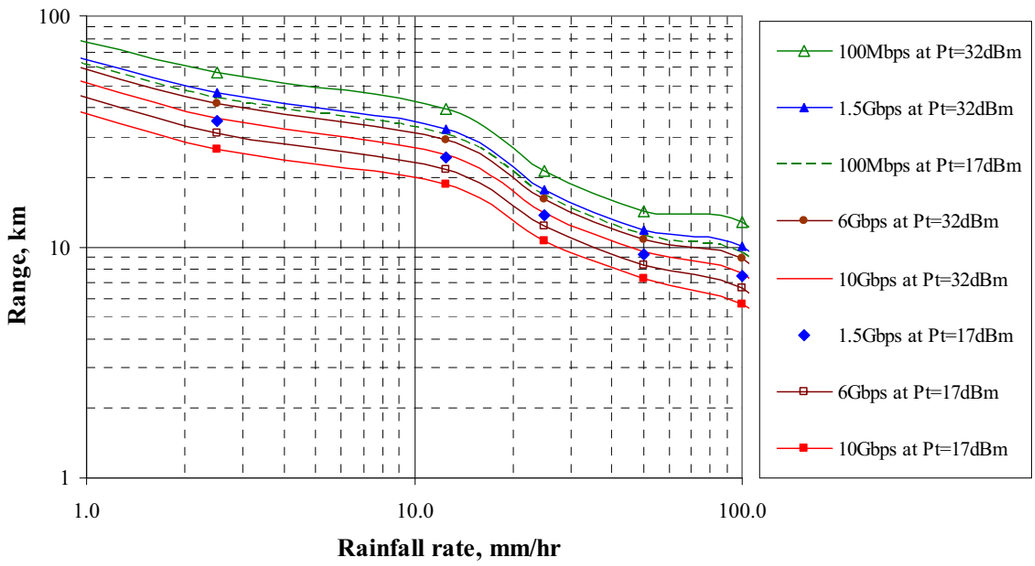

Fig. 12. Communication range of a typical E-band link versus rain fall rates. Carrier frequency is 83.5 GHz, vertical polarization, antenna gain 52 dBi.

4. Adaptive antenna arrays for future wireless communications

4.1 Spatial power combining arrays at mm-wave frequencies

With the advance in digital signal processing techniques, the adaptive antenna array is becoming an essential part of wireless communications systems (Guo, 2004; Mailoux, 2005). The use of adaptive antenna array for long range millimeter wave ad-hoc communication networks is particularly critical due to increased free space loss and reduced level of practically achievable output power. An ad-hoc or mobile network that relies on high gain antennas also requires beam scanning. The antenna beam can be steered to a desired direction with appropriate beam forming. Passive phased arrays generally suffer from losses in combining networks that are very high at the mm-wave frequencies. Active arrays with integrated power amplifier and antenna elements are effective in coherent spatial power combining increasing the total radiated power proportionally to the number of power amplifiers *N*. The advantages of spatial power combining are clearer at mm-wave frequencies because of the relatively low power and poor linearity of high-power amplifiers in these frequency bands. One way to overcome this problem is to use corporate power combining of multiple power amplifiers in parallel, as long as the incremental loss in the combining circuitry is less than the incremental

[7] ITU-R.P.837-5. Characteristics of precipitation for propagation modeling

gain of each additional power amplifier (York, 2001). As the electrical aperture and effective antenna gain is also proportional to the number of antenna array elements *N*, the effective isotropic radiated power (EIRP) is increased proportionally to N^2. Where the receive terminal is equipped with identical antenna array, an effective SNR increases proportionally to N^3 or more (due to reduction of the effective receiver noise dependent on the degree of the correlation). At the mm-wave frequencies, a phase-only beam steering becomes practical for this type of transmitting array since the size of a high EIRP array remains moderate. It can be shown that for a 1000-element array, the fractional bandwidth exceeds 7% at the scan angles within ±45°. This allows for a phase-only beam steering over the full 5 GHz wide RF channels available in the E-band.

We illustrate an advantage of an adaptive array over a fixed beam antenna with a simple example. With the reference link specification used in Figure 10, we replace a fixed beam antenna with a square lattice power combining array. Estimated communication range for the E-band ad-hoc link equipped with identical adaptive square lattice arrays of $N = n^2$ elements at both the transmit and receive RF terminals is shown in Figure 13 for practical scan angle from ±20° to ±45°, and typical propagation conditions. The transmitted power for each of the array elements is 15 dBm assuming that a single MMIC power amplifier with 1dB gain compression of 18 dBm is used for each array element and a -3 dB back off applied for the linearity required. A practical efficiency for the mm-wave antenna arrays is assumed of η=0.5. For clarity the carrier frequency is fixed at 73 GHz (in the lower E-band). Figure 13 shows that the medium to long communication range is achievable for the small to medium size arrays. It can be noted that the physical size of the array is very small. Thus, the aperture of the largest array shown in Figure 13 (n=64) is only a quarter of the aperture of a fixed beam antenna used in Figure 10.

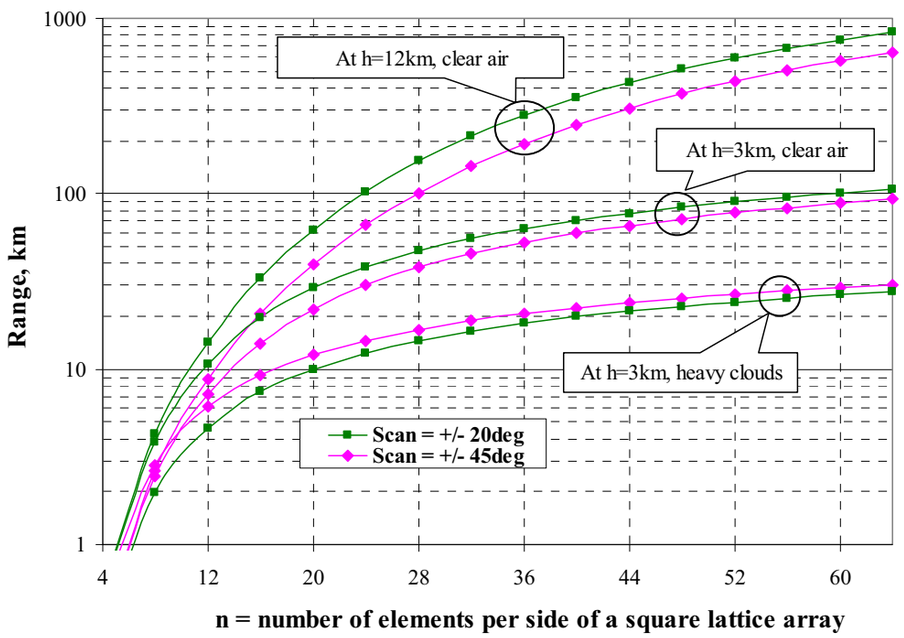

Fig. 13. Predicted communication range for a 73GHz link equipped with a square lattice power combining arrays for selected scan angles. Transmitted power is 15 dBm for each array element

For the chosen reference link parameters, a small power combining array with n = 16, N=256 elements (a linear size of 40 mm only) exhibits performance compatible with that of the link having a much larger (360mm) fixed beam antenna. A link equipped with a moderate size array, say n=36, that measures only 90 mm, is capable of the communication range beyond 100 km (at a favourable propagation conditions). Small antenna array size makes it very attractive for applications where the terminals are mounted on the mobile platforms (e.g. terrestrial and air born vehicles).

4.2 Challenges

As antenna elements must be spaced closely together (less than a half of the wavelength) to prevent grating lobes, practical realization of such antenna arrays poses a challenge due to the extremely tight space constraints at the mm-wave frequencies (about 2 mm in the E-band). The RF front end components, such as the low noise amplifier (or power amplifier), frequency converter, local oscillator (LO), as well as the intermediate frequency (IF) or baseband circuitry in the analogue signal chain should be tightly packed behind the antenna elements. With the current mm-wave integrated circuit technology, the practical implementation of such antenna arrays remains challenging. However, the recent progress in the CMOS and SiGe technology for the mm-wave applications (Cathelin et al., 2007; Floyd et al., 2007; Grass et al., 2007; Laskin et al., 2007; Pfeiffer et al., 2008; Reynolds et al., 2007) and advanced multi-chip module integration technologies (Posada et al., 2007) indicate that it becomes practical in the near future.

Although pure digitally beam forming allows the production of output signals with maximum SINR, ease of on-line calibration and generation of many antenna patterns simultaneously, it is impractical for the large wideband arrays due to two major reasons. Firstly, it is too costly since the cost of digital data processing is proportional to bandwidth and increases, at least, linearly with the number of elements. Secondly, the space constraints in the E-band make it very difficult to implement. Therefore, some degree of analogue (RF, LO or IF) beam forming is needed. This lowers the cost of digital electronics by a factor equal to the number of elements beam formed by analogue methods and also reduces the number of connections at the back of the antenna array. Thus, the area of a 4 by 4 sub-array with IF beam forming implemented in the E-band is about 100 mm^2 and it would provide a tight, but feasible accommodation for each the IF, LO, power and control circuits. A number of analogue sub-arrays can be controlled by a digital beam former to form a hybrid antenna array.

We have developed methods of adaptive beam forming for such hybrid arrays and built a small-scale prototype of the E-band communication system that implements an adaptive antenna array. The main functional block of the prototype is a four-channel dual-conversion receive RF module integrated with a linear end-fire steerable antenna array. Both receive and transmit modules use sub-harmonic frequency converters previously reported in (Dyadyuk et al., 2008a, 2008b). Phase and magnitude controls for each channel are implemented at IF using 6-bit phase shifters and attenuators. Both receive and transmit modules use the baseband frequency 1– 2 GHz that enables re-use of the digital modems developed earlier (Dyadyuk et al., 2007d). Bench test results of the receive and transmit modules have been reported in (Dyadyuk and Guo, 2009).

5. Conclusion

Enabling technologies for multi-gigabit spectrally efficient wireless communication systems in the E-band have been discussed. The performance of state-of-the-art E-band wireless communication system for high-capacity wireless networks has been evaluated. The analysis has been supported by experimental results on the prototypes. It has been shown that the performance of the fixed and ad-hoc mm-wave networks for existing and emerging applications can be further improved by implementation of the spatial power combining antenna arrays. The main challenges in the practical realization of the proposed systems have also been discussed.

6. Acknowledgment

The authors wish to acknowledge our colleagues R. Kendall, J. Pathikulangara, B. Murray, J. Joseph and D. Abbott for the digital modem development, X. Huang for a hybrid beam forming algorithm, J. W. Archer and O. Sevimli for the MMIC designs, A. Weily and N. Nikolic for the antenna designs, A. Grancea, R. Shaw, M. Shen, L. Stokes and J. Tello for their contributions to design, integration and testing of the prototypes.

7. References

Archer, J. W. and Shen, M. G. (2004). W-Band Transmitter Module Using Gallium Arsenide MMICs, *Microwave & Optical Tech. Letters,* vol. 42, no. 3, Aug. 2004, pp. 210-213, ISSN: 0895-2477

Cathelin, A.; Martineau, B.; Seller, N.; Douyere, S.; Gorisse, J.; Pruvost, S.; Raynaud, C.; Gianesello, F.; Montusclat, S.; Voinigescu, S.P.; Niknejad, A.M.; Belot, D.; Schoellkopf, J.P. (2007). Design for millimeter-wave applications in silicon technologies, *Proceedings of the 33rd European Solid State Circuits Conference,* pp. 464-471, Sep. 2007, Munich, Germany, ISSN: 1930-8833, ISBN: 978-1-4244-1125-2

Dyadyuk, V.; Stokes, L.; Sevimli, O. (2007a). A W-band multi-gigabit wireless link with high spectral efficiency, *Proceedings of* the *Intern. Joint Conf. of the TSMMW2007 and the MINT-MIS2007*, pp. 11-144, Feb. 2007, Seoul, Korea, Dongguk University, Seoul

Dyadyuk, V.; Sevimli, O.; Bunton, J. D.; Pathikulangara, J.; Stokes, L. (2007b). A 6 Gbps Millimeter Wave Wireless Link with 2.4 bit/Hz Spectral Efficiency, *Proceedings of the IEEE Intern. Microwave Symp. (IMS2007)*, pp. 471-474, June 2007, Honolulu, Hawaii, ISSN: 0149-645X, ISBN: 1-4244-0688-9

Dyadyuk, V.; Bunton, J. D.; Kendall, R.; Pathikulangara, J.; Sevimli, O.; Stokes, L. (2007c). Improved spectral efficiency for a multi-gigabit mm-wave communication system, *Proceedings of the 37th European Microwave Conf. (EuMC 2007),* pp. 810-813, Oct. 2007, Munich, Germany, ISBN: 978-2-87487-001-9

Dyadyuk, V.; Bunton, J. D.; Pathikulangara, J. et al, (2007d). A Multi-Gigabit Mm-Wave Communication System with Improved Spectral Efficiency, *IEEE Trans. on MTT, Vol. 55, Issue 12, Part 2,* Dec. 2007, pp. 2813-2821, ISSN: 0018-9480

Dyadyuk, V.; Archer, J. W.; Stokes, L. (2008a). W-Band GaAs Schottky Diode MMIC Mixers for Multi-Gigabit Wireless Communications, In: *Advances in Broadband Communication and Networks,* Agbinya, J. I. et al (Ed.), Chapt. 4, pp. 73-103, River Publishers, ISBN: 978-87-92329-00-4, Denmark

Dyadyuk, V.; Stokes, L.; Shen, M. (2008b). Integrated W-band GaAs MMIC Modules for Multi-Gigabit Wireless Communication Systems, *Proceedings of the 2008 Global Symposium on Millimeter Waves (GSMM 2008),* pp. 25-28, April 2008 Nanjing, China ISBN: 978-1-4244-1885-5

Dyadyuk, V. and Guo, Y. J. (2009). Towards Multi-Gigabit Ad-hoc Wireless Networks in the E-band, *Proceedings of the Global Symposium on Millimeter Waves (GSMM 2009),* paper 1569188415, Apr 2009, Sendai, Japan, Tohoku University, Japan

Floyd, B.; Reynolds, S.; Valdes-Garcia, A.; Gaucher, B.; Liu, D.; Beukema, T.; Natarajan, A. (2007). Silicon Technology, Circuits, Packages, and Systems for 60-100 GHz, *Proceedings of the IEEE Radio Frequency Integrated Circuits Symp. (RFIC2007), Workshop* "Millimeter-wave/Quasi–Millimeter-Wave Highly-Integrated Circuits", June 2007, Honolulu, Hawaii, ISSN: ISSN: 1529-2517, ISBN: 1-4244-0531-9

Grass, E.; Herzel, F.; Piz, M. (2007). 60 GHz SiGe-BiCMOS Radio for OFDM Transmission, *Proceedings of the 2007 IEEE Intern. Symp. On Circuits and Systems*, pp. 1979-1982, May 2007, New Orleans, ISBN: 1-4244-0920-9

Guo, Y. J. (2004). *Advances in Mobile Access Networks*, Artech House, ISBN: 1-58053-727-8, Boston, MA

Laskin, E.; Chevalier, P.; Chantre, A.; Sautreuil, B.; Voinigescu, S.P.(2007). 80/160-GHz Transceiver and 140-GHz Amplifier in SiGe Technology, *Proceedings of the IEEE Radio Frequency Integrated Circuits Symp. (RFIC2007),* pp. 153-156, June 2007, Honolulu, Hawaii, ISSN: 1529-2517, ISBN: 1-4244-0531-9

Mailloux, R. J. (2005). *Phased Array Antenna Handbook*, *Second Edition,* Artech House, ISBN: 1-58053-689-1, Boston, MA

Pfeiffer, U. R.; Mishra, C.; Rassel, R. M.; Pinkett, S.; Reynolds, S. K. (2008). Schottky Barrier Diode Circuits in Silicon for Future Millimeter-Wave and Terahertz Applications, *IEEE Trans. on MTT, Vol. 56, Issue 2, Feb.* 2008, pp. 364-371, ISSN: 0018-9480

Posada, G.; Carchon, G.; Soussan, P.; et al. (2007). Microstrip Thin-Film MCM-D Technology on High-Resistivity Silicon with Integrated Through-Substrate Vias, *Proceedings of the 37th European Microwave Conf. (EuMC 2007),,* pp. 1133–1136, Oct. 2007, Munich, Germany, ISBN: 978-2-87487-001-9

Reynolds, S. K.; Floyd, B. A.; Pfeiffer, U. R.; et al. (2006). A Silicon 60-GHz Receiver and Transmitter Chipset for Broadband Communications, *IEEE Journal of Solid-State Circuits*, vol. 41, 2006, pp. 2820-2831, ISSN: 0018-9200

Yong, S. K.; Chong, C. C. (2007). An Overview of Multigigabit Wireless through Millimeter Wave Technology: Potentials and Technical Challenges. *EURASIP Journal on Wireless Communications and Networking*, Vol. 2007 (2007), Article ID 78907, ISSN: 1687-1472, e-ISSN: 1687-1499

York, R.A. (2001). Some considerations for optimal efficiency and low noise in large power combiners. *IEEE Trans. on MTT,* Vol. 49, Issue 8, Aug. 2001, pp. 1477–1482, ISSN: 0018-9480

Mobile and Wireless Communications Network Layer and Circuit Level Design

Edited by Salma Ait Fares and Fumiyuki Adachi

ISBN 978-953-307-042-1
Hard cover, 404 pages
Publisher InTech
Published online 01, January, 2010
Published in print edition January, 2010

Mobile and wireless communications applications have a clear impact on improving the humanity wellbeing. From cell phones to wireless internet to home and office devices, most of the applications are converted from wired into wireless communication. Smart and advanced wireless communication environments represent the future technology and evolutionary development step in homes, hospitals, industrial, vehicular and transportation systems. A very appealing research area in these environments has been the wireless ad hoc, sensor and mesh networks. These networks rely on ultra low powered processing nodes that sense surrounding environment temperature, pressure, humidity, motion or chemical hazards, etc. Moreover, the radio frequency (RF) transceiver nodes of such networks require the design of transmitter and receiver equipped with high performance building blocks including antennas, power and low noise amplifiers, mixers and voltage controlled oscillators. Nowadays, the researchers are facing several challenges to design such building blocks while complying with ultra low power consumption, small area and high performance constraints. CMOS technology represents an excellent candidate to facilitate the integration of the whole transceiver on a single chip. However, several challenges have to be tackled while designing and using nanoscale CMOS technologies and require innovative idea from researchers and circuits designers. While major researchers and applications have been focusing on RF wireless communication, optical wireless communication based system has started to draw some attention from researchers for a terrestrial system as well as for aerial and satellite terminals. This renewed interested in optical wireless communications is driven by several advantages such as no licensing requirements policy, no RF radiation hazards, and no need to dig up roads besides its large bandwidth and low power consumption. This second part of the book, Mobile and Wireless Communications: Key Technologies and Future Applications, covers the recent development in ad hoc and sensor networks, the implementation of state of the art of wireless transceivers building blocks and recent development on optical wireless communication systems. We hope that this book will be useful for students, researchers and practitioners in their research studies.

How to reference

In order to correctly reference this scholarly work, feel free to copy and paste the following:

Val Dyadyuk, Y. Jay Guo and John D. Bunton (2010). Enabling Technologies for Multi-Gigabit Wireless Communications in the E-Band, Mobile and Wireless Communications Network Layer and Circuit Level Design, Salma Ait Fares and Fumiyuki Adachi (Ed.), ISBN: 978-953-307-042-1, InTech, Available from: http://www.intechopen.com/books/mobile-and-wireless-communications-network-layer-and-circuit-level-design/enabling-technologies-for-multi-gigabit-wireless-communications-in-the-e-band

INTECH
open science | open minds

InTech Europe
University Campus STeP Ri
Slavka Krautzeka 83/A
51000 Rijeka, Croatia
Phone: +385 (51) 770 447
Fax: +385 (51) 686 166
www.intechopen.com

InTech China
Unit 405, Office Block, Hotel Equatorial Shanghai
No.65, Yan An Road (West), Shanghai, 200040, China
中国上海市延安西路65号上海国际贵都大饭店办公楼405单元
Phone: +86-21-62489820
Fax: +86-21-62489821

IntechOpen

IntechOpen